

MICROSTRUCTURAL INTERACTIONS DURING CASTING AND ARTIFICIAL AGEING FOR A HYPOEUTECTIC A356 ALUMINIUM ALLOY WITH AG AND SC ADDITIONS

D. Bakavos, Supparerk Boontein and C. Limmaneevichitr

D. Bakavos, is with the Faculty of Engineering, Production and Engineering, King Mongkut's University of Technology Thonburi, 126 Pracha Uthit Road Bangmod Thungkhru, Bangkok 10140, Thailand

Contact E-mail: dimitrios.baka@kmutt.ac.th

ABSTRACT.

In this study an A356 hypoeutectic alloy modified with Ag and Sc separately has been studied. The results show that Sc additions it is crucial for as cast components however when it has been artificially aged to a T6 temper Sc exhibits a negative response to the hardness. In contrast the Alloy with Ag additions has demonstrated a subtle refining of Si eutectic enhancement of artificial ageing kinetics and strong resistance to overaging.

1. INTRODUCTION

Reduction of cost and high strength to weight ratio are two aspects of great importance, when it comes to select materials for automotive applications such as engine, chassis and civil airframe parts. To that end foundry aluminium alloys are considered as candidate materials because they offer production of near net to shape of complex components with high efficiency. Additionally artificial ageing to a T6 temper when it could be performed high strength could be obtained. In particular the A356 (Al-7.0%Si-0.3%Mg) hypoeutectic alloy due to its high strength, excellent castability, weldability, machinability and good corrosion resistance serve as the basis for aluminium material of choice when it comes to casting parts destined for transport applications (American Foundry Society, 2006).

The strength of the A356 in the as cast condition it is offered by its equilibrium microstructure after casting. Mainly it comes down to grain size, primary α -Al and Si eutectic particles. Various researcher groups try to modify its microstructure by adding to the melt exotic and not alloying elements such as: La, In, Eu, Se, Dy, Yb, Sc, Na, Sr etc. From the few that offers effective grain, α -Al refinement and Si eutectic modifications is the Sc, Sr etc (Nogita et al., 2004).

The use of Sc as alloying element in aluminium it has gained increased attention the last two decades. Three principal effects that can be attributed to Sc when it is added to aluminium alloys are: (a) grain and eutectic phase (Si in Al-Si-Mg) refinement during casting (b) precipitation hardening from Al_3Sc particles and (c) grain structure control from Al_3Sc dispersoids during recrystallization. However Sc potential to large extend it is depending on the aluminium system that is added and

based on this your target goal expected from Sc should be considered accordingly. When it is added to precipitation hardened wrought aluminium alloys there is a conflict when the strength is been maximized by precipitation hardening of Al_3Sc precipitates due to their high ageing temperatures needed for nucleation and growth for these phases and lower that needed for the Al_2Cu , Mg_2Si and Zn_2Mg in the 2xxx 6xxx and 7xxx aluminium systems respectively (Royset & Ryum, 2005).

Over and above the last years Ag alloying additions into 2xxx series wrought alloys with high or low Cu:Mg ratio has been expanded to 6xxx, 7xxx and 8xxx aluminium alloy systems. The use of Ag as the "must" alloying element addition is due to research findings that when Ag is added combined with artificial ageing, Ag enhances the age hardening response and radically affects the microstructural evolution. In the case of a 2139 alloy it inhibits the formation of $Cu\{001\}_{Al}$ GP zones and θ'' promoting the formation of Mg-Ag and Mg-Ag-Cu co-clusters as a result of enhancing the ageing kinetics and by replacing the θ' phase with Ω on the highly dense $\{111\}_{Al}$ planes increasing noticeably the strength after artificial ageing (Bakavos et al., 2008). However Ag additions has been overlooked as an important alloying element in cast hypoeutectic alloys of the Al-Si-Mg system. This fundamental research aims to understand the effect of Sc and Ag in the cast microstructure and ageing hardening behavior on a foundry A356 hypoeutectic alloy.

2. EXPERIMENT

2.1 Experimental Apparatus

The material used in this research was commercial Al-0.7Si-0.4Mg alloy (A356, wt % would be used throughout this article).

Table 1. Chemical compositions of the studied alloys.

Alloy	Si	Mg	Sc	Ag	Ti	Fe	Al
A	7.10	0.3	-	-	0.10	0.13	Bal.
B	7.10	0.3	-	0.4	0.09	0.11	Bal.
C	7.10	0.3	0.4	-	0.10	0.12	Bal.

The A356 ingots were made from primary aluminium to minimize any contamination effect from minor impurities. Table 1 shows the chemical composition of the A356 alloy ingot used in this work.

As received A356 material of batch size 1400 g was heated up to $750\text{ }^{\circ}\text{C} \pm 5^{\circ}\text{C}$ in a SiC crucible using a 12 kW induction furnace. Melts of A356 alloy were treated with Ag and Sc additions separately at the same level of 0.4% wrapped in aluminium foil and introduced to the melt. The chemical composition for Ag additions was based on to the Ag amount found in the commercial wrought aluminium aerospace alloy 2139 (Bakavos et al., 2008). Similar for Sc additions was based on the data which revealed optimal primary α -Al size and Si eutectic length refinement (Prukkanon et al., 2009). The melt was degassed by purging argon through a stainless steel tube (6mm in diameter) coated with zircon. The melt in each case was carefully skimmed to remove dross and other impurities. The chemical compositions of the cast alloys used in the study were determined by emission spectrometer (ARL-3460) and listed in Table 1. Subsequently the melt was gravity cast into a standard tensile tension test steel mold according to ASTM B557M-02a. In order to ease the melt flow the mold was preheated to a temperature of $250^{\circ}\text{C} \pm 5^{\circ}\text{C}$. The mold walls were coated with a refractory material belonging into the R_2O_3 type. The cooling rate determined from the data acquisition system was equal to $180\text{ }^{\circ}\text{C}/\text{min}$ or $3^{\circ}\text{C}/\text{sec}$. The microstructure of the as cast alloys were examined on cross sections by standard metallographic procedures.

Specimens of circular cross section and cylindrical geometry with dimensions of 2 cm x 3 cm (diameter x height) where solution treated (SHT) for 4 hrs at $540\text{ }^{\circ}\text{C}$ with a $5\text{ }^{\circ}\text{C}/\text{min}$ heating rate, water quenched at room temperature and subsequently aged at $170\text{ }^{\circ}\text{C}$ to T6 temper and beyond with a $75\text{ }^{\circ}\text{C}/\text{min}$ heating rate.

The microstructures for the as cast and after SHT samples were studied by means of optical microscopy using an Olympus GX51 optical microscope. For the selected aged specimens the precipitates were identified with means of transmission electron microscope TEM using the Titan HRTEM. A standard mechanical testing machine was used to test the materials after SHT and compare it to the as cast condition. Brinell hardness measurements were also performed utilizing a standard universal hardness testing machine with a 2.5mm in diameter indenter and an applied load of 62.5 kg for 10 sec. For each tensile testing condition and hardness measurement 5 minimum samples and hardness measurements were undertaken.

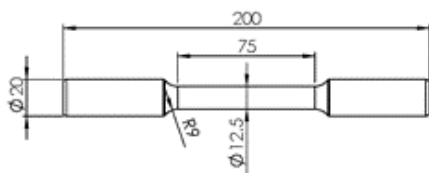


Fig. 1 Mechanical test sample geometry and dimensions.

3. ANALYSIS

3.1 As cast microstructure

Fig. 2 (a, c, e) shows the as cast microstructures observed in the three different conditions. α -Al dendrites and the

interdendritic network of the Al-Si eutectic phase typical of the conventionally cast hypoeutectic Al-Si alloys are identified in all the three alloys. Additionally to these the intermetallic π -Fe ($\text{Al}_8\text{Mg}_3\text{FeSi}_6$) with a Chinese script (green arrow) or blocky morphology (blue arrow) and intermetallic β -Fe plates (Al_5FeSi) (yellow arrow) were present. From the preliminary qualitative analysis of the optical microstructure there is a suggestion that the π -Fe phase with a Chinese script number density is higher in the C alloy when it is compared to the A and B alloy. Moreover there is another intermetallic phase present in the C alloy which is highlighted with the red arrow and is present in the alloys where Si and Sc is present (Royset & Ryum, 2005) the AlSi_2Sc_2 phase (red arrow).

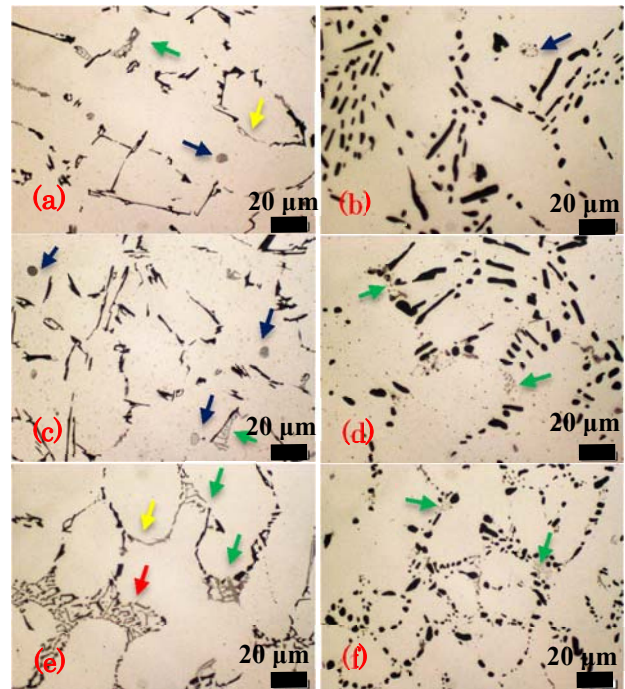


Fig. 2 optical microstructure for the as cast alloy A (a, b), B (c, d) and C (e, f). In the as cast state (a, c and e) and after solution heat treatment (b, d, f).

Additionally the average length of the Si eutectic in the as cast condition has been identified as 9.13, 7.21 and 4.31 μm for the A, B and C respectively. The Si eutectic in the A alloy has the typical coarse plate-like eutectic morphology with an average length of 9.13 μm and aspect ratio of 3.2 (see Fig. 3). For the B alloy the morphology of Si eutectic it is still dominated by plate like morphology however there are Si eutectic particles that show a plate like shape with rounded edges. In addition the average Si eutectic length has been found to be finer when it is compared to the Si eutectic particle length present in the A alloy. The average length recorded is approximately 7.21 μm with aspect ratio of 2.62 respectively. For the C alloy the Si eutectic has the finest mixture of plate-like and globular-fiber morphology but is more dominant the plate like morphology. The average length of the Si eutectic particles is $\sim 5.1\text{ }\mu\text{m}$ with a 2.42 μm aspect ratio. Therefore it is evident that Ag altering the nucleation and

growth of Si eutectic leading to finer Si eutectic particles. However at this stage the refining mechanism has not been fully understood and we could only speculate that Ag and Si particles are forming co-clusters and/or Ag-Si-Mg co-clusters which grows to Si eutectic. Similar phenomena it has been observed during early stages of precipitation in 2xxx alloy systems when Ag, Mg and Si present. Additionally Sc refines the coarse plate like Si eutectic size and alters finer plate/fiber towards a fibrous one for a cooling rate of 3°C/sec.

3.2 Solution heat treated microstructure

Fig. 2 (b, d, f) shows the microstructures of A, B and C samples solution treatment. The same phases observed in the as cast condition are present after SHT. However spheroidisation and coarsening of the Si eutectic now has taken place. For the C alloy this has a negative impact to the refining effect of Sc for the selected SHT condition. Furthermore the π -Fe has been partially dissolved in all three alloys and has transformed into β -Fe phase and Mg in solid solution in agreement with research findings for Al-7.0Si-30Mg (wt%) alloy after 10 min SHT at 530 °C (Sjolander & Seifeddine, 2014). The length of the particles has been decreased in every case because of breaking and spheroidising of Si eutectic plates. For the alloy A the new average particle length is 6.50 μ m and the aspect ratio 2.66. For the B alloy is 6.42 μ m and 2.22 aspect ratio and finally for the C alloy 3.9 μ m and 1.78 aspect ratio respectively.

Additions of Ag shows a subtle effect on Si eutectic morphology and length compared to the Si eutectic particles present on base Ag free A alloy. The Si eutectic particles in the C alloy exhibit a higher degree of circularity when it is compared to the A alloy. The globular morphology is the strongest on the C alloy. Particles with a shape factor ranging between 0.5-1.00 (1.00 circle) in the A alloy accounts for 30% in the B alloy 40% and for the C alloy 46% respectively. The Si eutectic particles with a shape factor ranging between 0.5-1.00 has increased for every alloy but is stronger in the C alloy with Sc additions. The degree of particle circularity after SHT in the A alloy is 46%, in the B alloy 60% and for the C alloy 74% respectively.

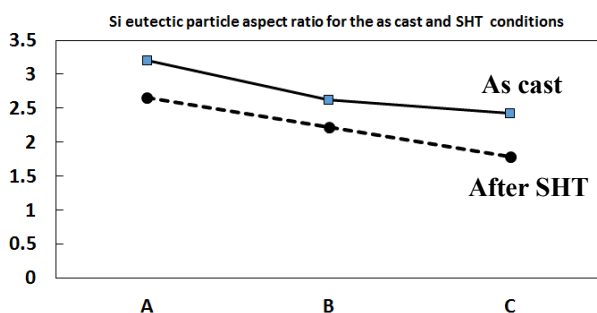


Fig. 3 Si eutectic particle aspect ratio for the (a) as cast samples (blue square solid line) and (b) after SHT treatment (black dotted line).

3.3 Mechanical properties (Cast vs SHT)

Fig. 4 shows the UTS for the as cast condition and after the solution treatment. For the as cast condition the C alloy has the highest tensile strength ~180 MPa, followed by the B alloy with 160 MPa and last the base A alloy with 150 MPa respectively. After solution heat treatment the alloy with the highest tensile strength is the alloy B which exhibits ultimate tensile strength ~220 MPa and followed from A and C with ultimate tensile strength of ~210 and 208 MPa respectively.

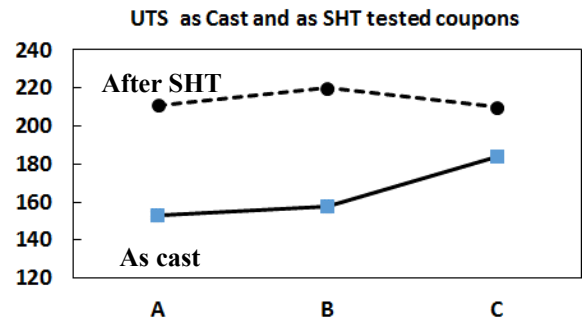


Fig. 4 UTS mechanical strength for the (a) as cast samples (black solid line) and (b) after SHT treatment (black dotted line).

After SHT the strength increase of alloy C is 18 % in comparison to the 40% and almost identical 38% for the B and A alloy respectively. The increase in strength observed at this stage could be explained by the dissolution of grain boundary and grain interior precipitates Mg_2Si that form during solidification releasing Mg and Si atoms into solution. Additionally the partially transformation-dissolution of intermetallic observed increase the Mg and Si content into the solution (see Fig. 2). However both A and B alloys exhibit double increase in strength compare to the C alloy. Therefore the result suggest that higher Mg content (which offers the highest solution strengthening contribution of any other alloying element in aluminium) solid solution has been taking place during SHT when it is compared to C.

The spheroidisation and particle coarsening of the Si eutectic could suggested as a contributing factor of strength increase for the A and B alloy. In contrast this effect it seems to have a negative impact on the Si eutectic refinement present for the C, Sc containing alloy. Moreover for the C alloy the higher intermetallic number density of phases present such π -Fe ($Al_8Mg_3FeSi_6$), $AlSi_2Sc_2$ and β -Fe (Al_5FeSi) respectively and their incomplete dissolution could also retain available solute into their structure and less into solution resulting in a smaller increase in mechanical strength.

3.4 Brinell Hardness profiles for a T6 temper

Fig. 5 shows the hardness profiles after artificial ageing to a T6 temper. The hardness profiles indicate that the alloy B shows enhanced ageing kinetics when it is compared to the alloy A and C. Alloy B reaches its peak strength after 4-8 hrs at isothermal ageing when for the B and C this is

achieved after 8-12 hrs. Furthermore the highest Brinell hardness is observed for alloy B ~115BH followed by alloy A ~105BH and alloy C ~100BH. After 48 hrs at temperature and beyond the peak ageing the alloy B exhibits flat hardness profile compare to Alloy A and C which its hardness is starting to reduce due to over ageing and precipitate coarsening.

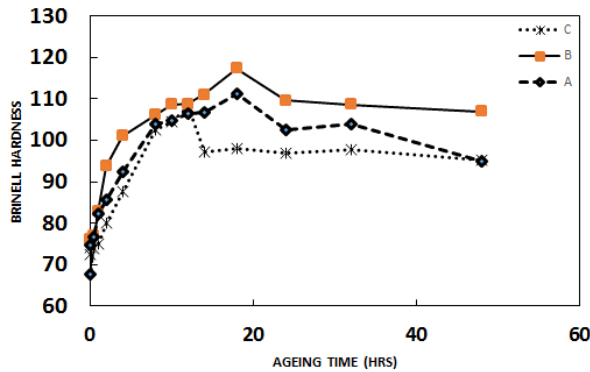


Fig. 5 Brinell ageing hardness profiles for the three alloys A, B, and C for a T6 temper.

The difference in hardness at 48 hrs artificial ageing could be explained from the microstructure present demonstrated in Fig. 6. Finer and higher number density of β''/β' precipitates are present in the B alloy compared to the A alloy.

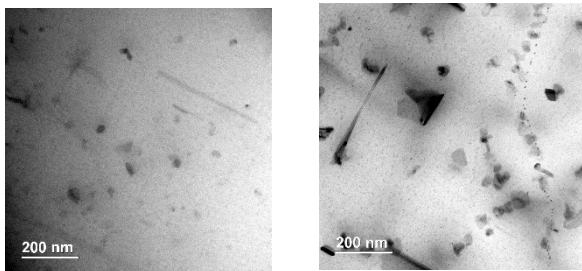


Fig. 6 BF TEM images taken close to $(100)_{Al}$ habit plane showing the precipitates present for (a) A and (b) B alloy after 48 hrs artificial ageing at 170 °C.

CONCLUSION

This study demonstrates the interactions of the alloying modification elements during casting and artificial ageing of a A356 hypoeutectic alloy. Alloy modifications with Sc result in a refine Si eutectic towards a mixture of plate/fibrous morphology this has as a result to a higher ultimate strength in the as cast condition. Ag additions in the cast condition slightly refine the Si eutectic. After 4 hrs SHT at 540 °C the alloy with higher strength is the one with Ag additions. After artificial ageing to a T6 temper the Alloy with Ag additions exhibits enhanced ageing kinetics and resistance to over ageing. The alloy with Sc additions has a negative impact in hardness.

REFERENCES

American foundry society technical Dept, Casting source

directory, Schaumburg, Illinois, *engineered solutions*, pp 30-34, 2006.

Kazuhiro Nogita, Stuart McDonald and Arne K. Dhale, eutectic modification of Al-Si alloys with rare earth metals, *Materials Transactions*, vol. 45, no.2, pp. 323-326, 2004.

J.Royset and N Ryum, scandium in aluminium alloys, *International materials reviews*, vol. 50, no. 1, pp. 19-44, 2005.

D. Bakavos, P.B.Prangnell, B. Bes, F. Eberl, The effect of silver on microstructural evolution in two 2xxx series Al-alloys with a high Cu:Mg ratio during ageing to a T8 temper, *Mater.Sci and Engi.A*, 491, pp 214-223, 2008.

W. Prukkanon, N. Srisukhumbowornchai, and C. Limmaneevichitr, *J.Alloys Compd.*, vol. 477, pp 454-60, 2009.

E. Sjolander and S. Seifeddine, Optimisation of solution treatment of cast Al-7.0Si-0.3Mg and Al-8.0Si-3Cu-0.5Mg alloys, *Met.and Mater.Trans. A*, vol. 45A, pp 1916-1927, 2014.



Dr. Dimitrios Bakavos received the B.E. (1999), M.Sc. (2000), M.Sc (2001) and PhD (2006) degrees in aerospace engineering, and Metallurgical Engineering from Liverpool and Manchester University.

He is a lecturer, Department of Production Engineering, King Mongkut's University of Technology Thonburi. His current interests include aluminum casting technology, and solid state welding of dissimilar alloys.



As. Prof Chaowalit Limmaneevichitr received the B.E. (1993), and Ph.D. (2000) degrees in Metallurgical Engineering from University of Wisconsin.

He is a Vice *President* for Student Development, King Mongkut's University of Technology Thonburi. His current interests include aluminum casting technology, and welding engineering.



Dr. Supparerk Boontein received the B.E. (1999), M.Sc (2002), and Ph.D. (2010) degree in materials technology from King Mongkut's University of Technology Thonburi.

He is a lecturer, Department of Production Engineering, King Mongkut's University of Technology Thonburi. His current interests include aluminum casting technology.